51st International Congress of Meat Science and Technology
August 7-12, 2005 – Baltimore, Maryland USA

A STUDY OF MUSCLE CELL MORPHOLOGY DURING *RIGOR MORTIS* MEASURED BY IMAGE ANALYSIS

Stine B. Balevik[1], Lars H. Stien[2] and Erik Slinde[1]*

Institute of Marine Research, P.O. Box 1870 Nordnes, N-5817, Bergen, Norway.
Department of Biology, University of Bergen, P.O. Box 7800, N-5020 Bergen, Norway.

Key Words: rigor mortis, image analysis, osmotic pressure, water transport

Introduction

After death, blood circulation in animals ceases, but the catabolic processes of the muscle cells (myofibers) continue as long as energy is available. Firstly, remaining oxygen is used up, followed by ATP-dependent anaerobic metabolism. This leads to accumulation of lactic acid and lowering of pH. When pH-level reaches a certain level, it interferes with the synthesis of ATP, eventually stopping it completely (Robb, 2001). The muscle cells enters *rigor mortis* when ATP level reaches a minimum (Currie & Wolfe, 1979). In rigor almost all of the myosin heads form cross-bridges to actin but in an abnormal, fixed and resistant way (Bendall, 1951; Marsh, 1953). This actomyosin complexes are often used to explain the rigidity or stiffness characterizing *rigor mortis* (Partmann, 1963). However, it is also agreed that rigor/stiffness is resolved without any changes of these bridges (Toyohara & Shimizu, 1988; Ando *et al*., 1991). Clearly, other factors must be introduced to fully explain rigor-stiffness.

Several studies show osmotic- and extracellular changes in postmortem muscle (Heffron & Hegarty, 1974; Winger & Pope, 1980-81; Oplatka, 1994; Veiseth *et al.*, 2004). This can be a potentially important factor contributing to rigor/stiffness (Slinde *et al.*, 2003; Balevik *et al.*, 2004). Slinde *et al.* (2003) suggests that rigor/stiffness is a result of high osmotic pressure, due to increased number of molecules within the cells. This causes water movement from inter- to intracellular space, and as a consequence the cells size and shape changes.

Objectives

The purpose of the present study was firstly to use image analysis to detect changes in the morphological shape of muscle cells at different stages postmortem. Secondly; to discuss any findings in relation to the theory presented by Slinde *et al.* (2003), and possibly strengthen the evidence of intramuscular water transport into the cells during rigor. Fish muscle from Atlantic salmon (*Salmo salar* L.) was selected as model, as the swimming muscle (M. lateralis) is very homogenous with regard to fibre- and connective tissue composition (Hultin, 1984).

Methodology

Histology: Muscle pieces, 0.5x0.5x0.5 cm^3 were cut from slaughtered Atlantic salmon, 1 (pre-rigor), 22 (in-rigor) and 72 (post-rigor) hours postmortem. The rigor/stiffness was observed by a finger technique as described by (Botta, 1994). Cross sectioned samples were stained with PAS (Periodic Acid Shiff) and examined by a light microscope (Leica DMR, Leica mikroskopie and Systeme GmbH, Wetzlar, Germany) x 10, and a digital camera (Olympus DP10, Olympus optical CO, GmbH, Hamburg, Germany). Pictures were downloaded to software Image ProPlus v. 4.0 (Media Cybernetics L.P., Silverspring, Maryland, U.S.A).

Image analysis of muscle cells: The colouring of the muscle-slides resulted in intensity images without any colour information. In general, the muscle cell borders and the neighbouring interior (in comparison) had a dark and a light pink colour respectively. In consequence the image analysis was performed on only the green colour-layer of the RGB-digital-image. Variation in both the light function and colour staining over individual slides were suppressed by background correction, also called flat fielding (Seul et al., 2000). The cell borders were segmented using a threshold value of T = 100. Skeletonizing was then used to achieve a one pixel thick representation of the cell borders (Gonzalez & Woods, 1992; Borgefors & Nyström, 1997). This initial automatic segmentation was followed by a manual segmentation, where a skilled researcher sanctioned which cells had been segmented correctly. Alternatively cell borders were added and/or corrected when necessary. The segmented cells were stored as circular lists representing the n polygon vertices of the cell border; $(i_0,j_0),\ldots,(i_k, j_k),\ldots,(i_n,j_n)$; $(i_0, j_0) = (i_n, j_n)$. Standard descriptive variables for each cell, as area, compactness and rectangularity, were calculated from these list representations (Sonka et al., 1998).

(1)

$$area = \frac{1}{2}\left|\sum_{k=1}^{n-1}(i_k\, j_{k+1} + i_{k+1}\, j_k)\right|$$

$$compactness = \frac{(borderlength)^2}{area}$$

$$rectangularity = \frac{area}{areaboundingrectangle}$$

The bounding rectangle is the rectangle of minimum area that bounds the cell region.

(2)

$$\alpha(i, j) = i\cos\theta + j\sin\theta \qquad \beta(i, j) = -i\sin\theta + j\cos\theta$$

This rectangle was found as the minimum and maximum of all boundary points (i_k, j_k) and directions θ (0-90°). Compactness = 1 for perfect circles. Rectangularity has values in the interval (0,1], with 1 representing a perfectly rectangular region. A fourth measurement, especially designed for this problem domain, was concavity.

(3)

$$concavity = \frac{convexarea - area}{area}$$

The *convexarea* is the area of the smallest convex region enveloping the respective cell region (Figure 1). The convex region can be computed efficiently from the circular list representation (see above) (Sklansky, 1982; Orlowski, 1985; Shin & Woo, 1986). If one imagines a region with an elastic border, the *concavity*-variable (3) measures how 'inflated' the region is, i.e. how outstretched the region border is. *Concavity* has possible values in the interval [0, ∞). A cell without any windings or concavities will have *concavity* = 0.

Statistics: The statistical procedures were performed using the SAS software package v.8.0.2. (SAS Institute Inc., Cary, North Carolina, USA). Least square means were calculated for each stage of rigor. T-tests were used to detect significant differences between LS-means. Effects of fish were also included in the model to avoid individual differences dominating the results. All *p*-values below 0.05 were considered significant. *P*-values above 0.20 were considered not significant (denoted n.s).

Results & Discussion

The shape of the muscle cells cut in- and post-rigor was significantly different to the shape of the muscle cells cut pre-rigor (Table 1). The area of the cells clearly increased from pre- to in- and post-rigor. Slinde *et al.* (2003) suggests that after death, glycogen is converted to glucose and further metabolised to lactate. In addition, other catabolic reactions such as proteolysis, lipolysis and enzymatic reactions also contribute to increased number of molecules within the cells. This increases the osmotic pressure (π= cRT) and generates a water transport into the cells (Figure 1). And as a result the cell area expands. The pre-rigor cells had an, in comparison to in- and post rigor cells, more wavy and concave border (Figure 2). Following Slinde's theory this is due to low osmotic pressure and relative modest water transport into the cells pre-rigor. The low pressure inside the cells is not able to expand the cell borders fully. In contrast, during rigor, high osmotic pressure causes water transport into the cells expanding the cell borders. The shape of in- and post-rigor cells is more inflated compared to pre-rigor cells (Table1, Figure 2). The cells became more compact (lower compactness values) and less concave (lower concavity values) during rigor. As a cell expands the concavities are filled out (Figure 1). A possible explanation for the increase in hardness according to Slinde *et al.* (2003) is that the cells now follow the surrounding connective tissue more closely. The release of hardness/stiffness post-rigor may therefore be explained by rupture of the muscle cell membranes as the muscle deteriorates postmortem.

It is important to be aware of that cutting, freezing and chemical treatment may have different effects on muscle samples pre-, in- and post-rigor. For instance, the PAS-staining of the muscle samples resulted in a pink colour pre-rigor, while the in- and post muscle samples became purple (Figure 2). This is probably due to the lowering of pH during rigor. Sampling techniques have been done systematically in all state of rigor. Because of this, artefacts may have been converted to "white noise". The result presented still support the theory by Slinde *et al.* (2003).

Conclusions

The image analysis successfully detected a change in cell-shape from concave to more inflated during rigor. This supports the theory suggested by Slinde *et al.* (2003) that there is an influx of water into the cells. It is however important to remember that rigor is a complex process. The above observed changes in muscle cell morphology may therefore only be on piece of the puzzle explaining muscle stiffness during *rigor mortis*.

References

Ando, M.,Toyohara, H.,Shimizu, Y., Sakaguchi, M., 1991. Postmortem tenderization of fish muscle proceeds independently of resolution of *rigor mortis*. Nipp. Suis. Gakk. 57, 1165–1169.

Balevik, S.B.,Botha, S.S.C.,Hoffmann, L.C., Slinde, E., 2004. The effect of intramuscular water fluid transport on *rigor mortis*, Proceedings from the 50th International Congress of Meat Science and Technology. Helsinki, Finland, pp. 7.

Bendall, J.R., 1951. The shortening of rabbit muscle during *rigor mortis*: Its relation to the breakdown of adenosine triphosphate and creatine phosphate and to muscular contraction. J. Physiol. 114, 71–88.

Borgefors, G., Nyström, I., 1997. Efficient shape representation by minimizing the set of centres of maximal discs/spheres. Pattern Recog. Lett. 18, 465–447.

Botta, J.R., 1994. Seafoods: Chemistry, Processing, Technology and Quality. Blackie Academic and Professional, 140–168 pp.

Currie, R.W., Wolfe, F.H., 1979. Relationship between pH fall and initiation of isotonic contraction in postmortem beef muscle. Can. J. Animal Sci. 59, 639–647.

Gonzalez, R.C., Woods, R.E., 1992. Digital image processing. Addison-Wesley Publishing Company, USA.

Heffron, J.J.A., Hegarty, P.V.J., 1974. Evidence for a relationship between ATP hydrolysis and changes in extracellular space and fibre diameter during rigor development in skeletal muscle. Comp. Biochem. Physiol. 49A, 43–56.

Hultin, H.O., 1984. Postmortem biochemistry of meat and fish. J. Chem. Ed. 67, 289–298.

Marsh, B.B., 1953. Shortening and extensibility in *rigor mortis*. Biochim. Biophys. Acta 12, 478–479.

Oplatka, A., 1994. The role of water in the mechanism of muscular contraction. FEBS Lett. 355, 1–3.

Orlowski, M., 1985. A convex hull algorithm for planar simple polygons. Pattern Recog. Lett. 18, 361–366.

Partmann, W., 1963. Postmortem changes in chilled and frozen muscle. J. Food Sci. 28, 15–27.

Seul, M.,O'Gorman, L., Sammon, M.J., 2000. Practical Algorithms for Image Analysis. Cambridge University Press, UK, 76–77.

Shin, S.Y., Woo, T.C., 1986. Finding the convex hull of a simple polygon in linear time. Pattern Recog. Lett. 19, 453–458.

Sklansky, J., 1982. Finding the convex hull of a simple polygon. Pattern Recog. Lett. 2, 79–83.

Slinde, E.,Roth, B.,Suontama, J.,Balevik, S.,Stien, L., Kiessling, A., 2003. The influence of intracellular osmolarity on *rigor mortis*. Proceedings, 49th International Congress of Meat Science and Technology. 2nd Brazilian Congress of Meat Science and Technology, 135–136.

Sonka, M.,Hlavac, V., Boyle, R., 1998. Image Processing, Analysis, and Machine Vision. Brooks/Cole publishing company, USA.

Toyohara, H., Shimizu, Y., 1988. Relation of the *rigor mortis* of fish body and the texture of the muscle. Nipp. Suis. Gakk. 54, 1795–1798.

Veiseth, E.,Shackelford, S.D.,Wheeler, T.L., Koohmaraie, M., 2004. Indicators of tenderization are detectable by 12 h postmortem in Ovine longissimus. J. Anim. Sci. 82, 1428–1436.

Winger, R.J., Pope, C.G., 1980–81. Osmotic properties of post-rigor beef muscle. Meat Sci. 5, 355–369.

Tables and Figures

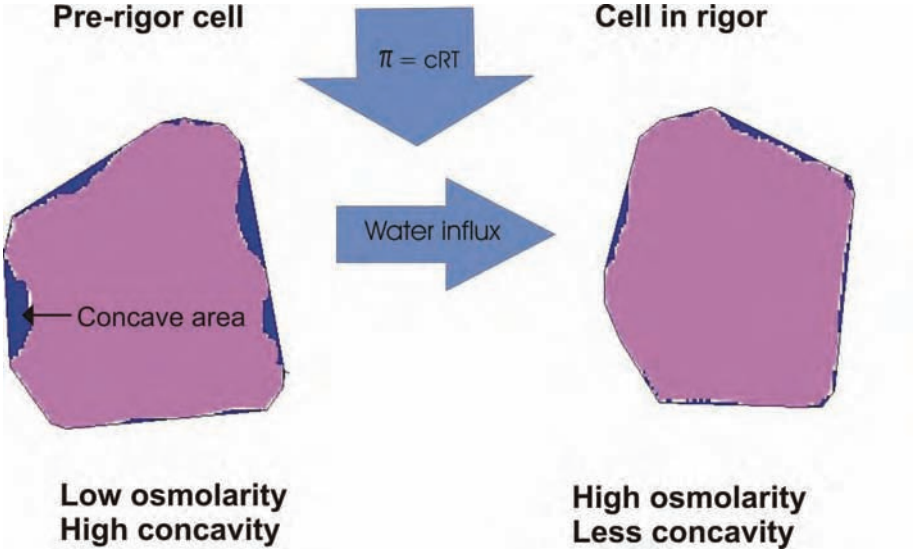

Figure 1. The covex area to a region is the least convex region containing the region. As the cell enters rigor, the osmotic pressure increases within the cell, π= cRT, and give rise to water transport into the cell. The cell expands and decreases its concavity.

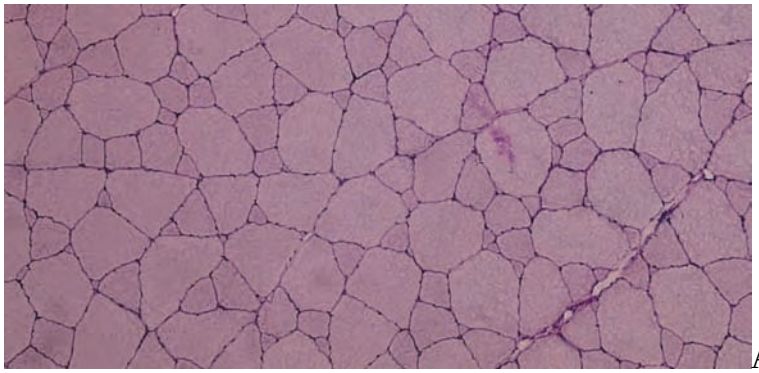

A. Pre-rigor

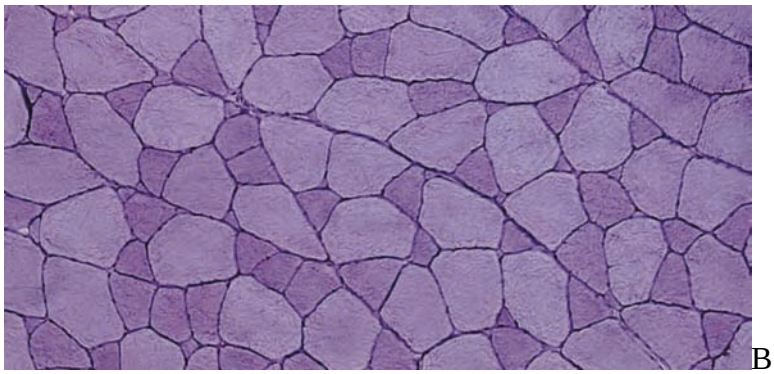

B. In rigor

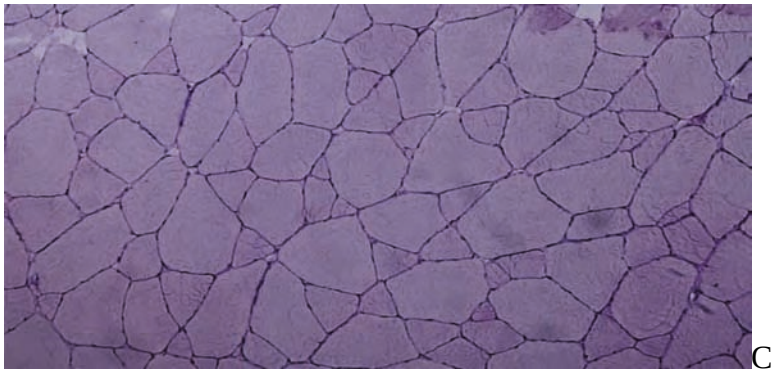

C. Post-rigor

Figure 2. Muscle cells in cross sections from white epaxial muscle of Atlantic salmon and stained with PAS. Picture A, B and C show muscle cells from pre-, in rigor and post-rigor state, taken 1, 22 and 72 hours after death respectively.

Variable	**Rigor-status**	**Pre-rigor**	**In-rigor**	**Post-rigor**
Area (μm^2)		12399 ± 395	14581 ± 452	14041 ± 447
	Pre-rigor		$p < 0.001$	$p = 0.006$
	In-rigor	$p < 0.001$		n.s
	Post-rigor	$p = 0.006$	n.s	
Compactness		19.552 ± 0.088	18.567 ± 0.100	18.455 ± 0.099
	Pre-rigor		$p < 0.001$	$p < 0.001$
	In-rigor	$p < 0.001$		n.s
	Post-rigor	$p < 0.001$	n.s	
Rectangularity		0.694 ± 0.003	0.709 ± 0.003	0.709 ± 0.003
	Pre-rigor		$p < 0.001$	$p < 0.001$
	In-rigor	$p < 0.001$		n.s
	Post-rigor	$p < 0.001$	n.s	
Concavity		0.066 ± 0.002	0.051 ± 0.002	0.046 ± 0.002
	Pre-rigor		$p < 0.001$	$p < 0.001$
	In-rigor	$p < 0.001$		$p < 0.084$
	Post-rigor	$p < 0.001$	$p < 0.084$	

Table 1. Statistical analysis of morphological variables of n = 1404 muscle cells in different state postmortem Least square means ± Standard Error for each rigor-status (in-, pre- and post-rigor) and *p*-values for differences of the least square means (t-test).